

# Equivalent rocking systems: Fundamental rocking parameters



**M.J. DeJong**

*University of Cambridge, United Kingdom*

**E.G. Dimitrakopoulos**

*The Hong Kong University of Science and Technology*

## SUMMARY

Early analytical investigations into the rocking behavior of structures assumed a simple model involving a single rigid rocking block on a rigid half-space. This paper investigates the use of rocking response spectra, analogous to linear elastic response spectra but instead derived from this simple rocking model, to predict the rocking response of more complicated structures. Fundamental rocking parameters are clarified, and examples of rocking spectra for trigonometric ground acceleration impulses are reviewed. Two specific rocking structures are addressed: the stone masonry arch and the stone masonry spire. Effective rocking parameters are derived for each of these structures, and the equivalence of the rocking response is investigated. Results indicate the utility of the fundamental rocking parameters for conducting a first order prediction of rocking response, although limitations are also discussed. While the focus is on masonry structures, the methodology applies to a wider class of structures which rock during earthquakes.

*Keywords: rocking, analytical dynamics, masonry, response spectra, near-field ground motion*

## 1. INTRODUCTION

The response of rocking structures to ground motion has long captured the fascination of researchers. The majority of this research has focused on the single rocking block, often inspired by the seminal work of Housner (1963), who developed a simple analytical model to describe rocking behavior. Subsequent research has involved experimental (e.g. Aslam et al. 1978), analytical (e.g. Yim et al. 1980, Zhang and Makris 2001), and computational techniques (e.g. Winkler et al. 1995), including advanced mechanical models which predict complicated bouncing, sliding and rocking behavior (e.g. Augusti and Sinopoli 1992, Lipscombe and Pellegrino 1993). While these studies effectively define rocking behavior, connecting rocking block theory with the response of real structures in earthquakes remains a significant challenge.

For elastic structures, a single degree of freedom (SDOF) linear elastic oscillator is typically used as the fundamental structure when determining the dynamic response. Earthquake engineers typically determine relevant mode shapes, and then use response spectra (derived using the SDOF elastic oscillator) to directly determine the seismic response. Use of the response spectra only requires the engineer to determine the natural frequency and damping of the structure.

In an analogous fashion, the aim of this paper is to investigate the use of rocking spectra, derived from the SDOF rocking block, to describe the response of more complex rocking systems. In particular, the paper will focus on two masonry structures which tend to rock during earthquakes: the masonry spire and the masonry arch. Being comprised of numerous blocks, each with multiple degrees of freedom, a major challenge is to determine how to simplify these complex structures as SDOF systems.

In addition, SDOF simplifications are only valid for limited ground motions, and can only predict global mechanisms and collapse. Thus, the focus will be on short duration pulse-type ground motions

which may be dominant in near-source earthquakes, and which are detrimental to rocking stability (Zhang and Makris 2001). More complex sliding, bouncing and rocking behavior between individual blocks, which may occur due to long-duration earthquake shaking, would have to be considered by other means.

In the following sections, the simple rocking block model proposed by Housner (1963) will be reviewed, along with a recent study (Dimitrakopoulos and DeJong 2012a) which proposes closed-form solutions for rocking response spectra for sinusoidal impulse ground motions. Subsequently, the analytical formulation for the masonry spire and the masonry arch will be presented, along with the parameters which govern rocking motion in each case. Finally, equivalent rocking structures will be discussed, along with the limitations of the approach.

## 2. SIMPLE ROCKING STRUCTURES

According to the formulation of Housner (1963), rocking motion is described by rotation about alternate bottom corners of the block in Fig. 1 (left). The equations of motion which describe this rocking about points O and O' can be written as:

$$\begin{aligned} I_O \ddot{\theta} + MgR \sin(+\alpha - \theta) &= -M\ddot{x}_g R \cos(+\alpha - \theta) \quad \rightarrow \quad \theta > 0 \\ I_{O'} \ddot{\theta} + MgR \sin(-\alpha - \theta) &= -M\ddot{x}_g R \cos(-\alpha - \theta) \quad \rightarrow \quad \theta < 0 \end{aligned} \quad (2.1)$$

where  $\ddot{x}_g$  is the horizontal ground acceleration,  $I_O$  is the mass moment of inertia of the block about point O,  $R$  and  $\alpha$  are defined in Fig. 1 (left), and  $\theta$  is the rocking angle with the positive rotation indicated. Note that rocking motion of the block does not commence until the ground acceleration exceeds a minimum magnitude, defined as:

$$\lambda = \frac{\ddot{x}_g}{g} = \tan \alpha \quad (2.2)$$

Rearranging Eqn. 2.1 and making use of the  $\text{sgn}()$  function yields:

$$\ddot{\theta} = p^2 \left( -\sin[\alpha \text{sgn}(\theta) - \theta] - \frac{\ddot{u}_g}{g} \cos[\alpha \text{sgn}(\theta) - \theta] \right) \quad (2.3)$$

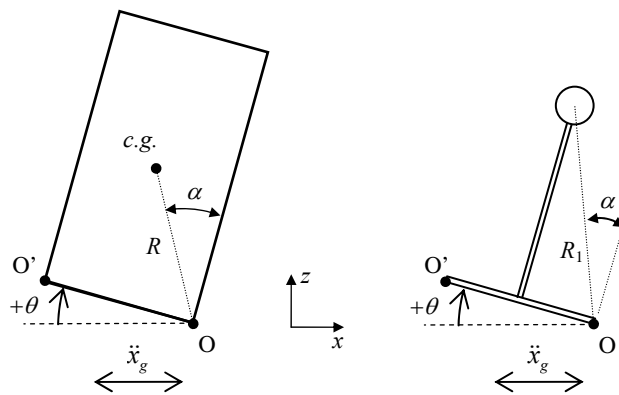


**Figure 1.** Geometry of two simple rigid rocking structures.

where  $p$  is the rocking frequency parameter, which is of critical importance. For the block in Fig. 1,  $p = \sqrt{3g/(4R)}$  and equals the pendulum frequency of the block when hung about its corner. For slender blocks, Eqn. 2.3 can be rewritten in linear form using small angle approximations:

$$\ddot{\theta} = p^2 \left( \theta - \alpha \operatorname{sgn}(\theta) - \frac{\ddot{x}_g}{g} \right) \quad (2.4)$$

In this case, again assuming small angles, the block commences rocking when  $\lambda = \alpha$ . Alternatively, the linearized equation of motion (Eqn. 2.4) can be obtained by using the following equation for small amplitude vibrations about the point of unstable equilibrium ( $\theta = \alpha$ ):

$$\frac{\partial^2 T}{\partial \dot{\theta}^2} \ddot{\theta} + \frac{\partial^2 V}{\partial \theta^2} \dot{\theta} = Q \quad (2.5)$$

where  $T$  and  $V$  are the kinetic and potential energy of the system, respectively, and  $Q$  is the generalized forcing function.

When the block returns to its initial position ( $\theta = 0$ ), impact occurs. Still according to the formulation of Housner (1963), the energy dissipated at impact can be estimated by conservation of angular momentum about the impacting corner. The energy dissipated is represented in the form of a coefficient of restitution,  $\eta$ , which defines the relative rotational velocities before and after impact. For the block in Fig. 1:

$$\eta = \frac{\dot{\theta}_{after}}{\dot{\theta}_{before}} = 1 - \frac{3}{2} \sin^2 \alpha \quad (2.6)$$

Clearly Eqn. 2.6 is a simplification of the actual behavior, which may not always be appropriate. Instead, the coefficient of restitution can be directly estimated, as is typically done in non-smooth dynamics formulations (e.g. Moreau 1988).

Equations 2.3 (or 2.4) and 2.6 completely define the rocking motion. Thus, the only structural parameters necessary to define the response of the rocking block are  $p$ ,  $\alpha$ , and  $\eta$ . Note that  $p$  has units of frequency, and in some way parallels the natural frequency for linear elastic oscillators. Similarly,  $\eta$  parallels the damping in the linear elastic system. However, linear elastic oscillators do not have a point of unstable equilibrium, so  $\alpha$  is an additional required parameter.

As mentioned in the introduction, there is a vast amount of literature on the single rocking block. For example, the authors of this paper derived closed-form solutions for the non-dimensional overturning envelopes and maximum rocking response for rocking blocks subjected to trigonometric impulses (Dimitrakopoulos & DeJong 2012a). A representative overturning envelope plot is presented in Fig. 2 (left). This plot defines the sinusoidal impulse characteristics (amplitude  $a_g$  and frequency  $\omega_g$ ) which will cause overturning of any rocking block (with the given coefficient of restitution) using only four equations (labelled Eqn. (i)-(iv) in Fig. 2). Approximate closed-form solutions were also derived for the maximum rocking response under sinusoidal impulses, and are of the following form:

$$\theta_{max} = \alpha \left[ 1 - \sqrt{1 - \eta^2 (1 - D_0^*)} \right] \quad \text{where} \quad D_0^* = f(a_g, \omega_g, \alpha, p) \quad (2.7)$$

where  $D_0^* = f(a_g, \omega_g, \alpha, p)$ . Eqn. 2.7 is plotted in Fig. 2 (right) for several coefficients of restitution, and compared with the exact response determined numerically. The curve for  $\eta = 0.9$  is essentially a

slice through the overturning plot in Fig. 2 (left) at the location indicated. Further details can be found in Dimitrakopoulos & DeJong (2012a), and similar semi-analytical solutions have also been derived for rocking systems with additional viscous damping (Dimitrakopoulos & DeJong 2012b), although these must be solved numerically.

In order to exploit the results in Fig. 2, and other existing literature regarding the single rocking block, it is useful to define other rocking system using equivalent parameters. For example, perhaps the simplest alternate rocking structure is the rocking point mass supported by rigid struts shown in Fig.1 (right). For this structure, the equations of motion (Eqn. 2.3 or 2.4) are unchanged. However, the frequency parameter is instead  $p = \sqrt{g/R_1}$ , the natural frequency of a simple pendulum, and the coefficient of restitution is instead  $\eta = 1 - 2\sin^2 \alpha$ . The critical angle of rotation is still  $\alpha$ . Using these new parameters, the results in Fig. 2 are directly applicable. In fact, these results are generally applicable for any rocking system which can be defined by the same rocking parameters. Thus, Fig. 2 (right) is effectively a rocking spectra, analogous to the standard linear elastic response spectra.

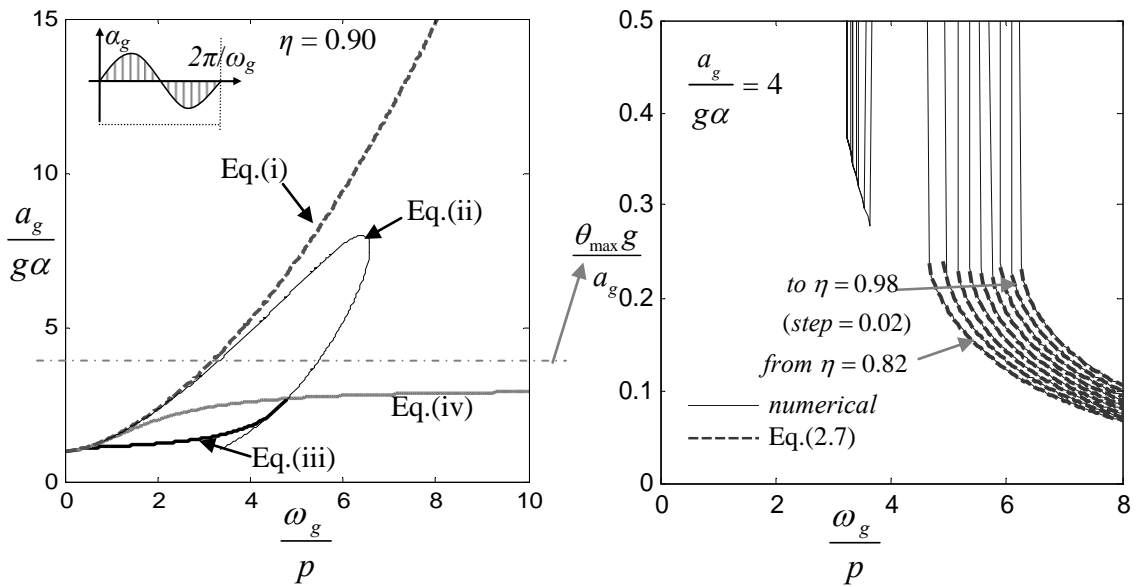


**Figure 2.** Non-dimensional rocking response due to a sinusoidal ground acceleration impulse: overturning envelopes defined by four curves labelled Eqn. (i)-(iv) (left), and rocking spectra for a range of  $\eta$  values (right).

### 3. ALTERNATIVE (COMPLEX) ROCKING STRUCTURES

The formulation for rocking structures presented above can be used to predict the seismic response of a variety of more complex structures. This section focuses on masonry structures, but the formulation could be applied to a wider array of rocking system.

#### 3.1. The Masonry Spire

Stone masonry spires are often extremely slender, and thus vulnerable to overturning during earthquakes. Even in the UK, which has only moderate seismic risk, severe spire damage or overturning is not uncommon. The analytical modeling presented here is part of a larger study on masonry spires (DeJong 2012, DeJong & Vibert 2012).

While the stone masonry spire is comprised of multiple blocks, assume first that the spire can be modeled as a conical shell which rocks about its base (Fig. 3a). If applied for an infinite duration, the fraction of horizontal to vertical ground acceleration required to overturn the hollow conical shell is:

$$\lambda_{hc} = \tan \alpha = \frac{3r_b}{H} \quad (3.1)$$

where the geometry is defined in Fig. 3a. Note that this value is 1.5 times greater than for the rocking block. Also, as for the rocking block,  $\lambda_{hc} = \alpha$  when applying small angle assumptions. The rocking parameter  $p$  is defined by:

$$p^2 = \frac{g}{H} \frac{\sqrt{\frac{1}{9} + \kappa^2}}{\left(\frac{5}{4}\kappa^2 + \frac{1}{6}\right)} \quad (3.2)$$

where  $\kappa = r_b / H$ . Additionally, the coefficient of restitution becomes:

$$\eta = 1 - \frac{\frac{1}{9} + \kappa^2}{\frac{5}{4}\kappa^2 + \frac{1}{6}} (1 - \cos 2\alpha) \quad (3.3)$$

Eqns. 2.3 and 2.4 still hold, and can be used to define the rocking response of the conical shell (neglecting rotation about the vertical axis). However, in reality, masonry structures crack diagonally when loaded laterally (Ochsendorf et al. 2004), making it necessary to refine the model. Assuming that a diagonal crack forms at the base of a solid spire tip and that a reflecting rocking mechanism results (Fig. 3b), new rocking parameters can be defined. The equations for these parameters become more extensive (not shown), but the resulting parameter values are presented in Fig. 4 for varying slenderness values ( $r_b / H$ ). Note that the effect of thickness is negligible, so Fig. 4 displays the relevant parameters for the entire range of typical spire geometries.

The exact spire geometry (i.e. the diagonal crack angle) must still be determined, but this is addressed in DeJong (2012) and compared with computational and experimental results in DeJong & Vibert (2012). Regardless, the fundamental equations from section 2 are applicable (for the assumed analytical model), as are the overturning and response spectra in Fig. 2.

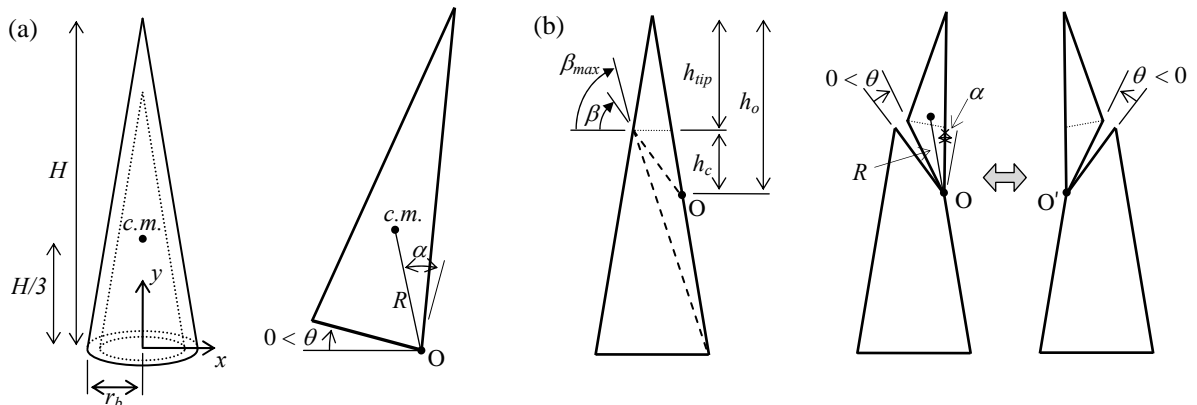


**Figure 3.** Assumed geometry and rocking mechanisms for two masonry spire models: (a) hollow conical shell, and (b) conical spire with diagonal cracking below a solid spire tip.

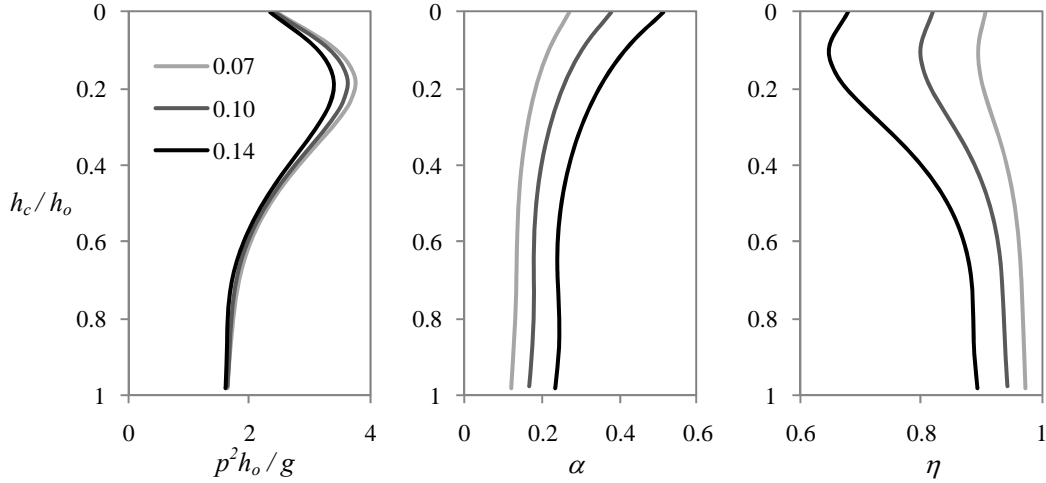


**Figure 4.** Rocking parameters for masonry spires of varying  $r_b / H$  which crack diagonally below a solid tip (see Fig. 3b).

### 3.2. The Masonry Arch

The masonry arch also rocks due to ground motion. Although the exact dynamic response involves a complicated interaction between multiple blocks, Oppenheim (1992) proposed a SDOF analytical model to capture the global rocking response (see Fig. 5). This model was extended and used effectively to predict experimental rocking arch collapse due to earthquake loading by DeJong et al. (2009).

Oppenheim (1992) assumed that the masonry arch could be modeled as a SDOF four-bar mechanism, allowing the rocking response to be described by the following equation of motion:

$$M(\theta)r\ddot{\theta} + L(\theta)r\dot{\theta}^2 + F(\theta)g = P(\theta)\ddot{x}_g \quad (3.4)$$

where  $\ddot{x}_g$  is the horizontal ground acceleration,  $r$  is the centre-line arch radius,  $\theta$  is the rotation angle in Fig. 5 (left), and the coefficients  $M(\theta)$ ,  $L(\theta)$ ,  $F(\theta)$ , and  $P(\theta)$  are nonlinear in  $\theta$ . In addition,  $\phi$  is defined as the rotation angle with respect to the initial geometry ( $\phi = \theta_0 - \theta > 0$ ). A similar equation describes rocking in the negative direction (Fig. 5, right). Finally, a coefficient of restitution  $\eta$  is required at impact. This can again either be derived from conservation of momentum equations, as outlined in De Lorenzis et al. (2008), or directly specified as an independent parameter.

The equation of motion for a four-bar mechanism (e.g. Eqn. 3.4) is highly nonlinear. However, typical arch geometries can sustain relatively small rotations before reaching the point of unstable equilibrium, i.e. the critical rotation angle. Thus, the use of linearized equations for small rocking amplitudes may describe arch rocking with reasonable accuracy. If so, use of linearized equations would allow definition of rocking parameters which make use of rocking block results.

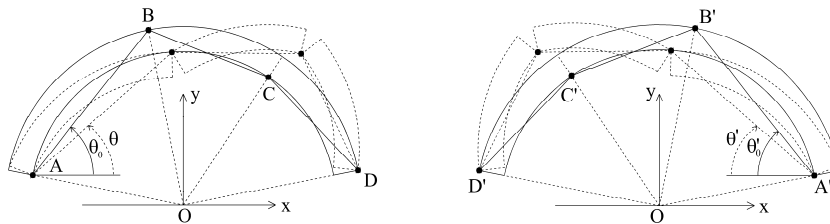


**Figure 5.** Assumed reflecting SDOF rocking arch mechanism.

Using Eqn. 2.5, the equation of motion for the rocking arch, linearized about the point of unstable equilibrium ( $\phi = \alpha$ ), becomes:

$$I_{eq} \ddot{\phi} - gG_{eq} (\phi - \alpha) = -B_{eq} \ddot{x}_g \quad (3.5)$$

where  $\phi$  is the rocking rotation defined above and the coefficients  $I_{eq}$ ,  $G_{eq}$ , and  $B_{eq}$  are constants derived directly from the arch geometry. Eqn. 3.5 can be rearranged to yield:

$$\ddot{\phi} = p^2 \left( \phi - \alpha \operatorname{sgn}(\phi) - a_{scale} \frac{\ddot{x}_g}{g} \right) \quad (3.6)$$

where:

$$p = \sqrt{\frac{gG_{eq}}{I_{eq}}} \quad ; \quad a_{scale} = \frac{B_{eq}}{G_{eq}} \quad (3.7)$$

Eqn. 3.6 is similar to the linearized equation of motion of the rocking block, with the exception of the  $a_{scale}$  term. This term results from a primary difference in the rocking systems. And, although Eqn. 3.7 provides viable equations to predict the response, an alternate method of defining  $a_{scale}$  is proposed using the following dynamic boundary conditions of the system:

$$\begin{aligned} \phi = 0; \quad \ddot{\phi} = 0 &\Rightarrow \ddot{x}_g = \lambda g \\ \phi = \alpha; \quad \ddot{x}_g = 0 &\Rightarrow \ddot{\phi} = 0 \end{aligned} \quad (3.8)$$

where  $\lambda$  is again the horizontal acceleration necessary to initiate motion. Meeting the boundary conditions in Eqn. 3.8 results in a revised definition of  $a_{scale}$ :

$$a_{scale} = \frac{\alpha}{\lambda} \quad (3.9)$$

Note that, using Eqn. 3.9,  $a_{scale} = 1$  for the linearized rocking block, and therefore does not appear in Eqn. 2.4. Thus, an additional parameter is necessary to define rocking systems in which  $\lambda \neq \alpha$ . Thus, three new fundamental rocking parameters have been defined for the rocking arch, and are plotted in Fig. 6. Note that the values for  $p$  assume  $r = 10$  m, but the plots for  $\alpha$  and  $a_{scale}$  are generally applicable as they do not depend on scale. A coefficient of restitution is also needed (not shown), but this is unchanged from previous studies.

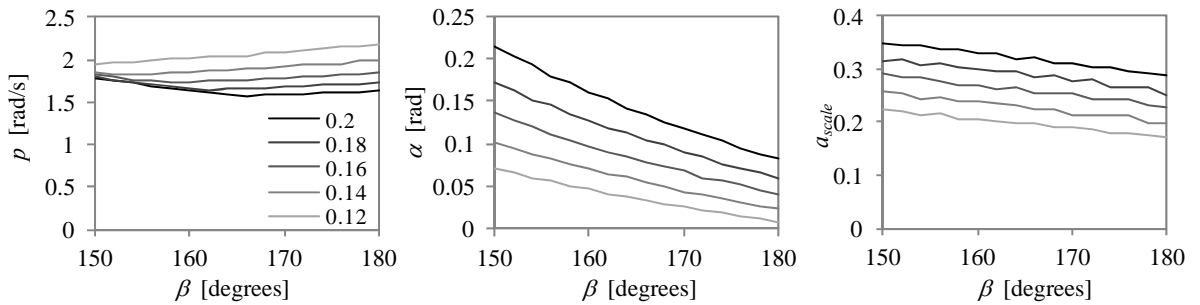


**Figure 6.** Arch rocking parameters for a range of arch geometries: arch inclusion angle,  $\beta = 150^\circ - 180^\circ$ , arch thickness to radius ratio,  $t_a / r = 0.12 - 0.2$ .

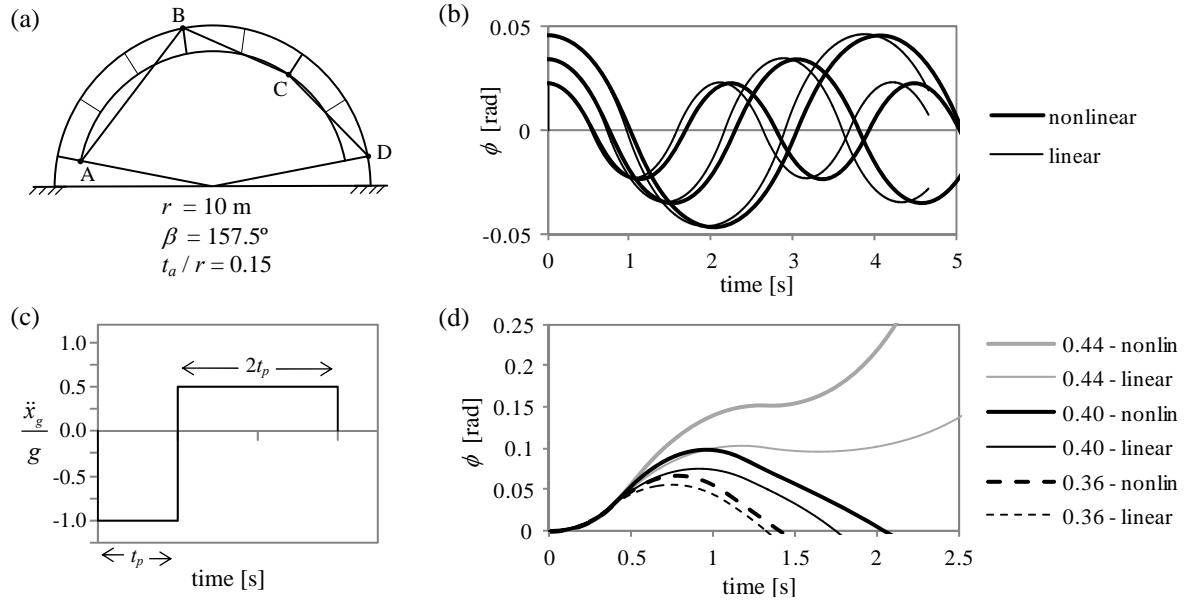


**Figure 7.** Comparison of linear and nonlinear arch rocking formulation: (a) arch geometry and mechanism, (b) free rocking response, (c) applied impulse, and (d) impulse response for  $t_p = 0.36, 0.40, 0.44$ .

A comparison between the nonlinear arch rocking response (Eqn. 3.4) and the linearized rocking response (Eqns. 3.6 and 3.9) is shown for the arch investigated by Oppenheim (1992) in Fig. 7. The free rocking response of the arch released from a given rocking angle is shown in Fig. 7b. The free rocking response is independent of  $a_{scale}$ , and thus the accuracy of the frequency parameter  $p$  (Eqn. 3.7) can be evaluated independently. The results from the nonlinear and linear formulations compare reasonably well, with the rocking frequency predicted by the linear formulation being slightly higher.

The linear and nonlinear predictions are compared in Fig. 7d for the impulse shown in Fig. 7c. The rocking rotations again compare reasonably well. Note that the prediction is worse if the block nears the point of instability, as the response become more nonlinear in that region. While a more complete evaluation of the accuracy of the linear formulation is ongoing, these initial results indicate that the linear formulation is more than adequate when considering the uncertainty of earthquake loading magnitude and the simplifications made to derive the SDOF analytical model.

### 3.3. Equivalence of the Rocking Response

The use of non-dimensional parameters allows a single solution to the rocking equations of motion to describe the rocking response of completely different structures to different ground impulses. For example, Fig. 8 shows the response of three rocking structures (Fig. 8a) to sinusoidal impulses of different magnitudes and frequencies (Fig. 8b). In Fig. 8c, the dimensional responses are quite different, but the non-dimensional responses collapse to a single curve due to the equivalent dimensionless terms shown. Thus, it is again evident how the rocking response spectra, derived from the response of the single rocking block, can be used to predict the response of more complex structures.

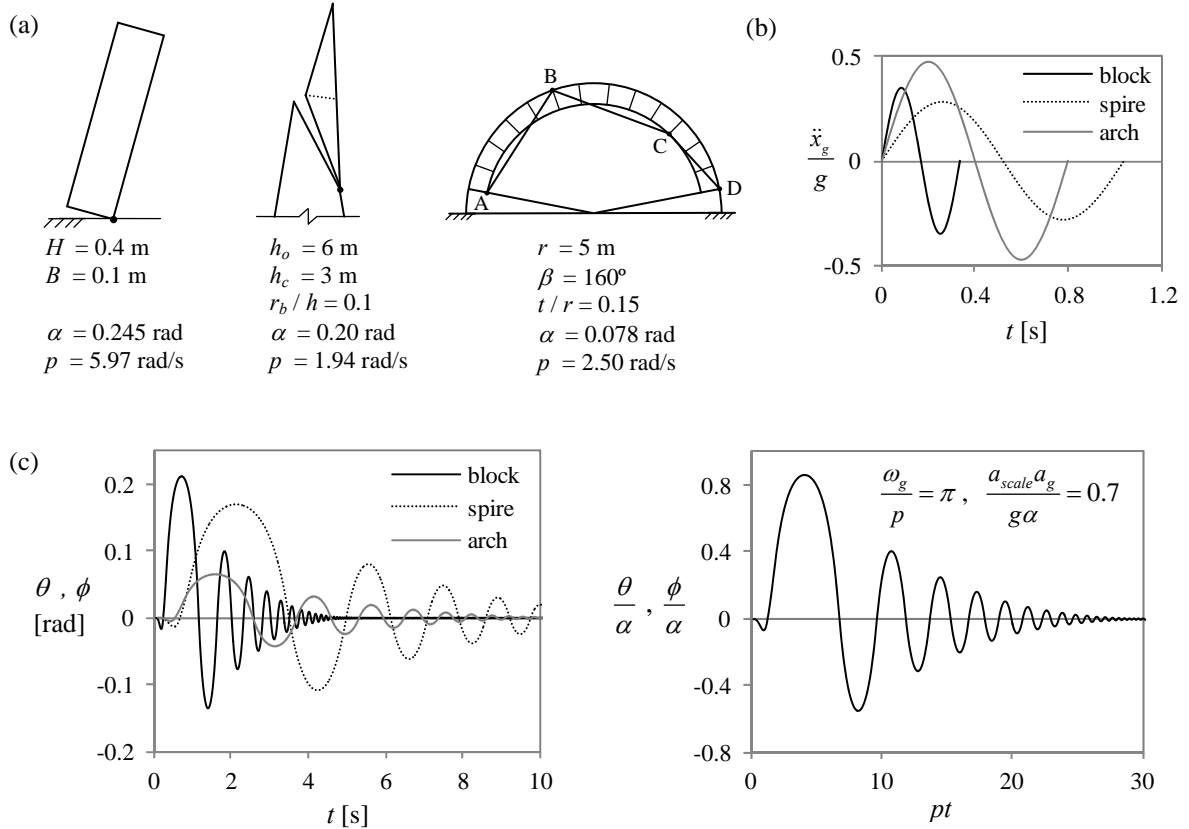


**Figure 8.** Comparison of rocking response: (a) three different structure with noted geometries, (b) applied impulse for each structure, (c) dimensional response, and (d) identical non-dimensional response.

## 5. CONCLUSIONS

Rocking spectra, derived from the rocking response of the single block (as in Fig. 2), have been shown to be applicable to both the masonry spire and the masonry arch. In the process, four parameters have been shown to be necessary to predict the linearized rocking response:  $p$ ,  $\alpha$ ,  $\eta$ , and  $\lambda$ . Thus, a rocking equivalent to the linear elastic response spectra, for structures which can be described as SDOF mechanisms, has been exemplified.

Clearly there are limitations to the approach described above. It must be emphasized that the intent is to quickly determine the approximate magnitude of global rocking response, not to predict precise displacements. Even the rocking response of a single block is quite sensitive to slight changes in ground motion for long duration rocking (e.g. Yim et al. 1980), particularly if the structure is small relative to the magnitude of shaking. However, for near-source records, where the magnitude of strong shaking is short (i.e. similar to an impulse), and for relatively larger structures which are less sensitive to high-frequency acceleration spikes, prediction capabilities are more robust. Thus, while predicting local displacement and damage to individual stones in a masonry structure is impossible, a reasonable prediction of global rocking is feasible, and has proved effective when compared to experimental and computational modeling results (DeJong et al. 2008, DeJong and Vibert 2012).

The formulation above is also limited to structures for which elastic effects can be assumed minimal, as is often the case for masonry structures which are relatively stocky. However, a similar approach can be applied for more flexible rocking structures (e.g. bridge piers), for which elastic effects may not be negligible. Such structures are explored by Acikgoz & DeJong (2012a,b).

## AKNOWLEDGEMENT

Financial support for aspects of this research was provided by the Engineering and Physical Sciences Research Council of the United Kingdom under grant reference number EP/H032657/1.

## REFERENCES

- Acikgoz, S. and DeJong, M.J. (2012a). The interaction of elasticity and rocking in flexible structures allowed to uplift. *Earthquake Engineering and Structural Dynamics* (published on-line, doi: 10.1002/eqe.2181).
- Acikgoz, S. and DeJong, M.J. (2012b). Characterizing the vulnerability of flexible rocking structures to strong ground motions. *15<sup>th</sup> World Conference on Earthquake Engineering*, Lisbon, Portugal.
- Aslam, M., Godden, W.G. and Scalise, D.T. (1978). Rocking and overturning of rigid bodies to earthquake motions, *LBL-7539*, Lawrence Berkeley Laboratory, University of California, Berkeley.
- Augusti, G. and Sinopoli, A. (1992). Modeling the dynamics of large block structures, *Meccanica* **27:3**, 195-211.
- Bray, J. D. and Rodriguez-Marek A. (2004). Characterization of forward-directivity ground motions in the near-fault region. *Soil Dynamics and Earthquake Engineering* **24:11**, 815– 828.
- Dimitrakopoulos, E.G. and DeJong, M.J. (2012a). Revisiting the rocking block: Closed form solutions and similarity laws. *Proceedings of the Royal Society A* (published on-line, doi: 10.1098/rspa.2012.0026).
- Dimitrakopoulos, E.G. and DeJong, M.J. (2012b). Overturning of retrofitted rocking structures under pulse-type excitations. *ASCE Journal of Engineering Mechanics* (published on-line, doi: 10.1061/(ASCE)EM.1943-7889.0000410).
- DeJong, M.J. (2012). Seismic response of stone masonry spires: Analytical Modeling, *Engineering Structures* (published on-line, doi: 10.1016/j.engstruct.2012.03.010).
- DeJong, M.J., De Lorenzis, L., Adams, S. and Ochsendorf, J. (2008). Rocking stability of masonry arches in seismic regions. *Earthquake Spectra* **24:4**, 847-865.
- DeJong M.J. and Vibert C. (2012). Seismic response of stone masonry spires: Computational and experimental modeling, *Engineering Structures* (published on-line, doi: 10.1016/j.engstruct.2012.03.001).
- De Lorenzis, L., DeJong, M.J. and Ochsendorf, J. (2007). Failure of masonry arches under impulse base motion. *Earthquake Engineering & Structural Dynamics* **36**, 2119-2136.
- Housner, G.W. (1963). The behavior of inverted pendulum structures during earthquakes. *Bulletin of the Seismological Society of America* **53:2**, 403-417.
- Lipscombe, P.R. and Pellegrino, S. (1993). Free rocking of prismatic blocks, *ASCE Journal of Engineering Mechanics* **119:7**, 1387-1410.
- Moreau, J.J. (1988). Unilateral contact and dry friction in finite freedom dynamics. In J.J. Moreau, P.D. Panagiotopoulos (Eds.), *Nonsmooth Mechanics and Applications*, CISM Courses and Lectures No. 302, pp. 1-82. Wien, New York: Springer-Verlag.
- Ochsendorf, J.A., Hernando, J.I., and Huerta S. (2004). Collapse of masonry buttresses. *ASCE Journal of Architectural Engineering* **10:3**, 88-97.
- Winkler, T., Meguro, K. and Yamazaki, F. (1996). Response of rigid body assemblies to dynamic excitation, *Earthquake Engineering and Structural Dynamics* **24:10**, 1389-1408.
- Yim, C. S., Chopra, A. K. and Penzien, J. (1980). Rocking response of rigid blocks to earthquakes. *Earthquake Engineering & Structural Dynamics* **8:6**, 565–587.
- Zhang, J. and Makris, N. (2001). Rocking response of free-standing blocks under cycloidal pulses. *Journal of Engineering Mechanics* **127:5**, 473-483.